Scientific Research Publishing

World Journal of Mechanics, 2025, 15(6), 105-115
https://www.scirp.org/journal/wjm
ISSN Online: 2160-0503
ISSN Print: 2160-049X

$e^{-}e^{+}$ Pair Production Using High Energy

Yara Owaidh Althurwi, Sadah Abdullah Alkhateeb, Nada Ahmad Almuallem

Department of Mathematics and Statistics, Faculty of Science, University of Jeddah, Jeddah, Saudi Arabia
Email: Yara5524@gmail.com

How to cite this paper: Althurwi, Y.O., Alkhateeb, S.A. and Almuallem, N.A. (2025) $e^{-}e^{+}$ Pair Production Using High Energy. *World Journal of Mechanics*, **15**, 105-115.
https://doi.org/10.4236/wjm.2025.156006

Received: June 1, 2025
Accepted: June 27, 2025
Published: June 30, 2025

Abstract

This work studies the energy distribution of pair production for Be_4^9 and Al_{13}^{25} using the Bethe-Heitler equation. We use the mathematics program "Mathematica" to compare the electromagnetic effects of photons interacting with beryllium and aluminum nuclei. We compare the impact of electric and magnetic cross-sections on pair generation. Using graphs, we investigate how electric and magnetic fields affect the production of $e^{-}e^{+}$. We also study the impact of atomic mass on $e^{-}e^{+}$ emission. Our results indicate that harnessing magnetic interactions can produce $e^{-}e^{+}$ with specific properties at high energies (MeV) and for lighter nuclei, the efficiency of electron-positron pair production increases significantly. We will now discuss this phenomenon in detail, illustrating the impact of energy and nuclear mass on pair production, as well as the role of multipole interactions in enhancing production efficiency. These ideas are crucial to PET technology, because regulated $e^{-}e^{+}$ pair formation and annihilation are fundamental to imaging efficacy. These ideas are particularly relevant to positron emission tomography (PET), because regulated electron-positron pair formation and extinction are fundamental to imaging efficacy.

Keywords

Pair Production, Bethe-Heitler Equation, Energy Distribution, Cross Section

1. Introduction

There are numerous particles in nature. They are split into Fermions and Bosons. Fermions are divided into leptons and quarks [1]. The electron is charged with Leptons, and the positron is the antiparticle of the electron, having the same mass as the electron but an equal opposite (positive) charge [2]. The electron was discovered in 1897 by J. J. Thomson [3], and Anderson discovered the positron in 1932 [2]. Nishina and others [4], Bethe, and Heitler [5] were the first to theorize who the theoretical treatment of ($e^{-}e^{+}$) pair photon production in 1934. In 1936,

Jaeger and Hulme [6] demonstrated that pair production Differential Cross-section (DCS) calculations yield better results at high incident photon energies. In 1947, A. D. Sakharov studied the interaction of the electron and the positron in pair production [7]. A further advance in pair production theory was the work of Davies and Bethe (1952), Bethe and Maximon (1954), and Davies *et al.* (1954), Some wide-angle electron-positron pair production measurements by Blumenthal *et al.* (1966), Asbury *et al.* (1967) and Alvenslaben *et al.* (1962). More recently, Tseng (1997) used a relativistic partial-wave method to examine pair production polarization correlations for intermediate-energy incident photons [8]. Hubbell [8] provides a historical overview of the ($e^{-}e^{+}$) by photons from Dirac's prediction of the position in 1928 until 2006. The (DCS) results for ($e^{-}e^{+}$)-Hubbell and Seltzer [9] revealed photon-based pair production.

There is a lot of scientific research on this topic. In 2020, Alkhateeb studied the effect of nuclear magnetic distribution on photon production of longitudinally polarized lepton pairs in the fields of Be_4^9 and Al_{13}^{25} nuclei [10]. In 2022, Alkhateeb, Alshaery, and Aldosary studied leptonic pair production in an electromagnetic field [11]. Finally, in 2024, Miroslav Pardy studied electron-positron pair production in Modern Quantum Electrodynamics [12]. Furthermore, the use of positron emission tomography (PET) in medical imaging in the 1970s demonstrated the practical applications of pair production, extending beyond theoretical physics [13].

In this study, the effect of high energies and the mass of the nucleus on the electron-positron pair production process using the Be_4^9 and Al_{13}^{25} nuclei will be studied. The study utilizes electromagnetic fields and high-energy effects on two nuclei, Be_4^9 and $Al_{13}^{25,}$ to produce a pair of $e^{-}e^{+}$, as well as mass effects to create a pair of $e^{-}e^{+}$. We apply the Beth-Heitler radiation equation to the pair production process at different incidence angles and high energies. This equation enables us to calculate the pair production rate as a function of photon energy and incidence angles. We will focus on studying the relationship between electron-positron pair production and photon collision energy, as well as the effect of photon projection angles on light nuclei. We will study the production of electron-positron pairs using the Beth-Hitler radiation equation and apply a mathematical program to generate graphs of this process. We will then analyze and examine the results in detail.

2. Formulation of the Problem

Our study focuses on how high energies affect electron-positron pair production through interactions with light nuclei, specifically Beryllium and Aluminum and studies the effect of mass for Beryllium and Aluminum nucleus on the electron-positron pair production process. In this work, we focus not only on the general effect of energy on electron-positron pair production but also on how high-energy levels enhance the efficiency of the process. Additionally, we examined the effect of nuclear mass, showing how the mass of the Beryllium and Aluminum nuclei significantly impacts the production rate of electron-positron pairs. The theoret-

ical framework of our study is based on the Bethe-Heitler equations, which describe the fundamental mechanisms of electron-positron pair production. These equations were implemented using the Mathematica program to obtain results and to compare the influence of both energy and nuclear mass on the electron-positron pair production process.

3. Research Methodology

In this section, we discuss the interaction of a photon with Be_4^9 and Al_{13}^{25} nuclei produces pairs of e^-e^+. The e^-e^+ process produced by the interaction of the γ-photon field with the nuclei field (N) can be written as **Figure 1**:

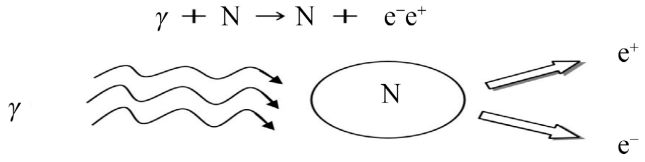

Figure 1. Simplified representation of a beam of high-energy photons colliding with a nucleus, resulting in the production of an electron-positron pair [11].

Also, the Depicts the Feynman diagrams for the issue of e^-e^+ pair production in the Electromagnetic field of the nuclei has presented in the following diagram **Figure 2**:

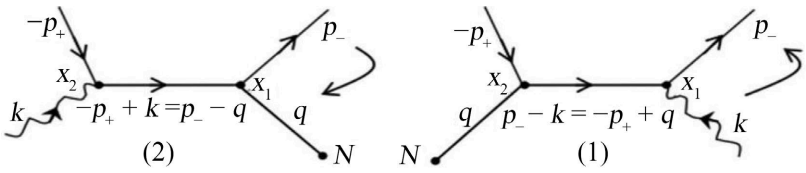

Figure 2. Feynman diagrams for the e^-e^+ pair production process [11].

In addition, the Bethe-Hitler equation for the electron-positron pair production process can be presented as follows: [10] [14] [15]

$$dBH = \frac{Z^2 \propto^3}{(2\pi)^2}\frac{|p_-||p_+|dE_+}{\omega^3}\frac{d\Omega_- d\Omega_+}{|q|^4}\left[\frac{p_-^2\sin^2\theta}{(E_- - p_-\cos\theta_-)^2}\left(4E_+^2 - q^2\right)\right.$$
$$-\frac{p_+^2\sin^2\theta_+}{(E_+ - p_+\cos\theta_+)^2}\left(4E_-^2 - q^2\right) + 2\omega^2\frac{p_+^2\sin^2\theta_+ + p_-^2\sin^2\theta}{(E_+ - p_+\cos\theta_+)(E_- - p_-\cos\theta_-)} \quad (1)$$
$$\left.-\frac{2p_+p_-\sin\theta_+\sin\theta_-\cos\phi}{(E_+ - p_+\cos\theta_+)(E_- - p_-\cos\theta_-)}\left(2E_+^2 - 2E_-^2 - q^2\right)\right]$$

This equation is the Bethe-Hitler equation for the electron-positron pair production process, and it can be written in an abbreviated form so that it is applicable using the following symbols:

$$d(\theta, Ze, \mu_1, Q, \Omega) = \mathrm{d}\sigma_{0e}(\theta) + d\mathrm{d}\sigma_{0m}(\theta) + \mathrm{d}\sigma_{0q}(\theta) + \mathrm{d}\sigma_{0\Omega}(\theta). \quad (2)$$

$$\mathrm{d}\sigma_{0e}(\theta) = 8\pi\eta\phi_{0e}(\theta)d\Omega, \quad (3)$$

$$\mathrm{d}\sigma_{0m}(\theta) = 8\pi\eta\left(\frac{\mu_1}{Ze}\right)^2 a_\mu \phi_{0m}(\theta) d\Omega, \tag{4}$$

$$\mathrm{d}\sigma_{0q}(\theta) = 8\pi\eta\left(\frac{\Omega}{Ze}\right)^2 a_q \phi_{0q}(\theta) d\Omega, \tag{5}$$

$$\mathrm{d}\sigma_{0\Omega}(\theta) = 8\pi\eta\left(\frac{\Omega}{Ze}\right)^2 a_\Omega \phi_{0\Omega}(\theta) d\Omega, \tag{6}$$

where

$$\eta = \left(\frac{Z^2 \propto^3}{4\pi^2}\right)\frac{p_+ p_- dE_+}{\omega^3}, \Delta_0 = (1 - cos\theta),$$

$$p_+ = \left|\overrightarrow{p_+}\right|, p_- = \left|\overrightarrow{p_-}\right|,$$

$\omega = E_+ + E_-$, ω is the energy of the colliding photon.

The Ze, μ_1, Q and Ω are electric charge $d\sigma_{oe}$, magnetic dipole $d\sigma_{om}$, electric quadrupole $d\sigma_{oq}$, and magnetic octupole $d\sigma_{o\Omega}$ moments of the target nucleus, respectively. The $\phi_{0e}(\theta)$, $\phi_{0m}(\theta)$, $\phi_{0q}(\theta)$ and $\phi_{0\Omega}(\theta)$ in the case of high energy E, $E' \gg m_0c^2$ [10] [14] [15]. Also, we obtain the values of $\phi_{0e}(\theta)$, $\phi_{0m}(\theta)$, $\phi_{0q}(\theta)$ and $\phi_{0\Omega}(\theta)$ from research [11].

4. Result and Discussion

In this section, we will discuss the effect of high energies on the e^-e^+ pair production process, as well as the impact of nuclear mass on this process.

4.1. Study the Effect of Different Energies and Angels for Be_4^9 and AL_{13}^{25} Nucleus on the e^-e^+ Pair Production Process

By use (1 - 6) equations such that the $d\sigma_{oe}$ represent the electric charge, $d\sigma_{om}$ represent the magnetic dipole, $d\sigma_{oq}$ represent the electric quadrupole and $d\sigma_{o\Omega}$ represent the magnetic octupole, total electric dE, and total magnetic dM. Differential Cross Section for the electron-positron pair production using formulas for the energy distribution is obtained for the nuclei Be_4^9 and AL_{13}^{25} at different values of incident photon energies ε = (500, 700, 900) MeV, where m = $0.910940637872524 \times 10^{-27}$ mass of electron.

Figure 3 shows the differential cross-sections Electric Charge $d\sigma_{oe}$, Magnetic Dipole $d\sigma_{om}$, Electric Quadrupole $d\sigma_{oq,}$ and Magnetic Octupole $d\sigma_{o\Omega}$ for the Be_4^9 nucleus.

From Figure 3 we notice that:

- The differential cross-sections electric charge $d\sigma_{oe}$ for Be_4^9 nuclei are increasing with decrease the photon energy but $d\sigma_{oe}$ increases with an increase in the incident photon angle. For example:

  The highest value at $\varepsilon = 500MeV$ and $\theta = 120^\circ$.
- The differential cross-sections magnetic dipole $d\sigma_{om}$ for Be_4^9 nuclei are increasing with decrease the photon energy but $d\sigma_{o\mathrm{m}}$ increases with increase the incident photon angle. For example:

The highest value at $\varepsilon = 500MeV$ and $\theta = 120^{\circ}$.

- The differential cross-sections electric quadrupole $d\sigma_{oq}$ for Be_4^9 nuclei are increasing with increase the photon energy but $d\sigma_{oq}$ increases with increase the incident photon angle. For example:

The highest value at $\varepsilon = 900MeV$ and $\theta = 120^{\circ}$.

- The differential cross-sections magnetic octupole $d\sigma_{o\Omega}$ for Be_4^9 nuclei are increasing with increase the photon energy but $d\sigma_{o\Omega}$ increases with decrease the incident photon angle. For example:

The highest value at $\varepsilon = 900MeV$ and $\theta = 60^{\circ}$.

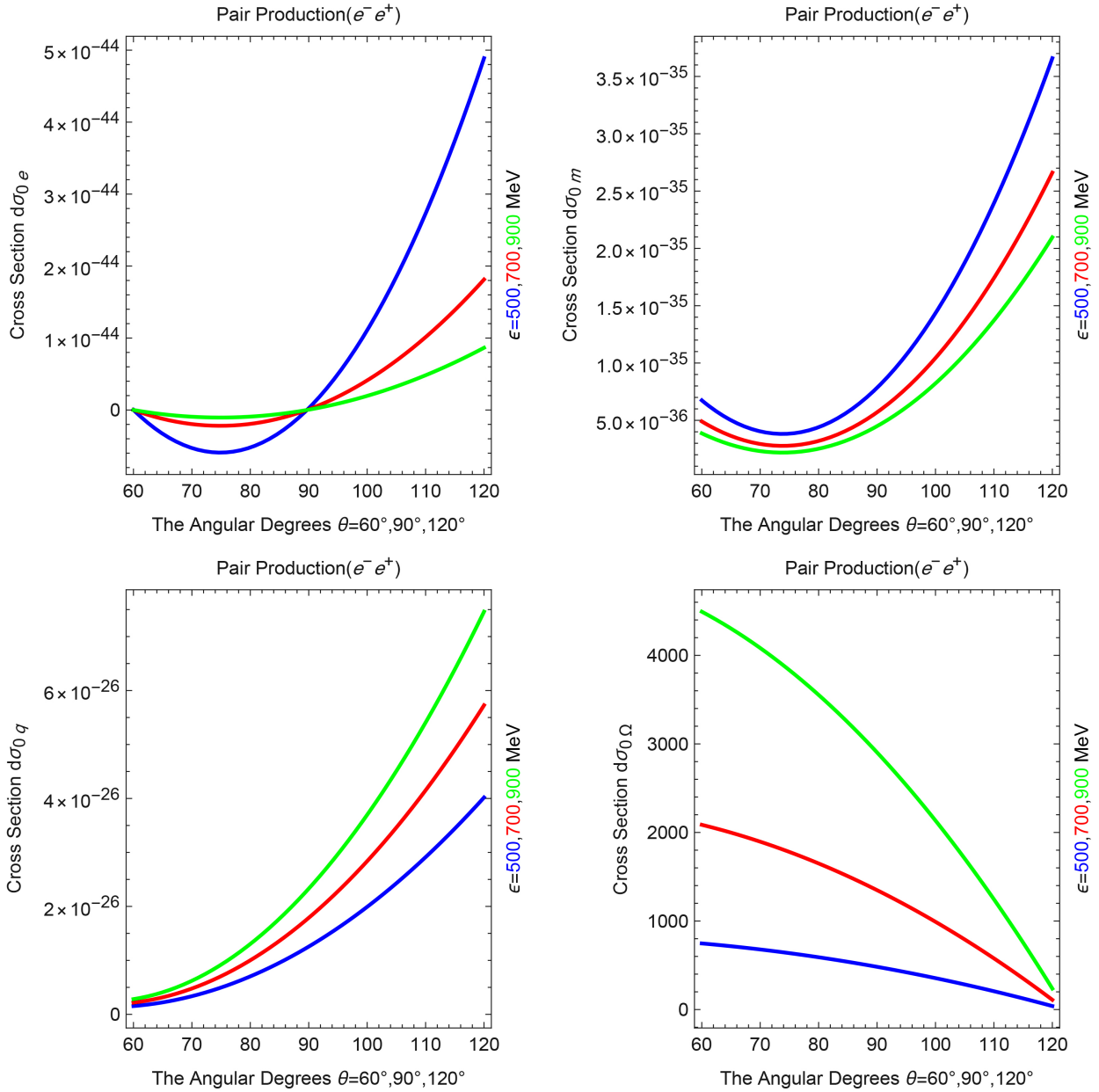

Figure 3. The DCS Electric Charge $d\sigma_{oe}$, Magnetic Dipole $d\sigma_{om}$, Electric Quadrupole $d\sigma_{oq}$ and Magnetic Octupole $d\sigma_{o\Omega}$ for the Be_4^9 nuclei.

Figure 4 depicts the differential cross-sections Electric Charge $d\sigma_{oe}$, Magnetic Dipole $d\sigma_{om}$, Electric Quadrupole $d\sigma_{oq}$ and Magnetic Octupole $d\sigma_{o\Omega}$ for the AL_{13}^{25} nuclei.

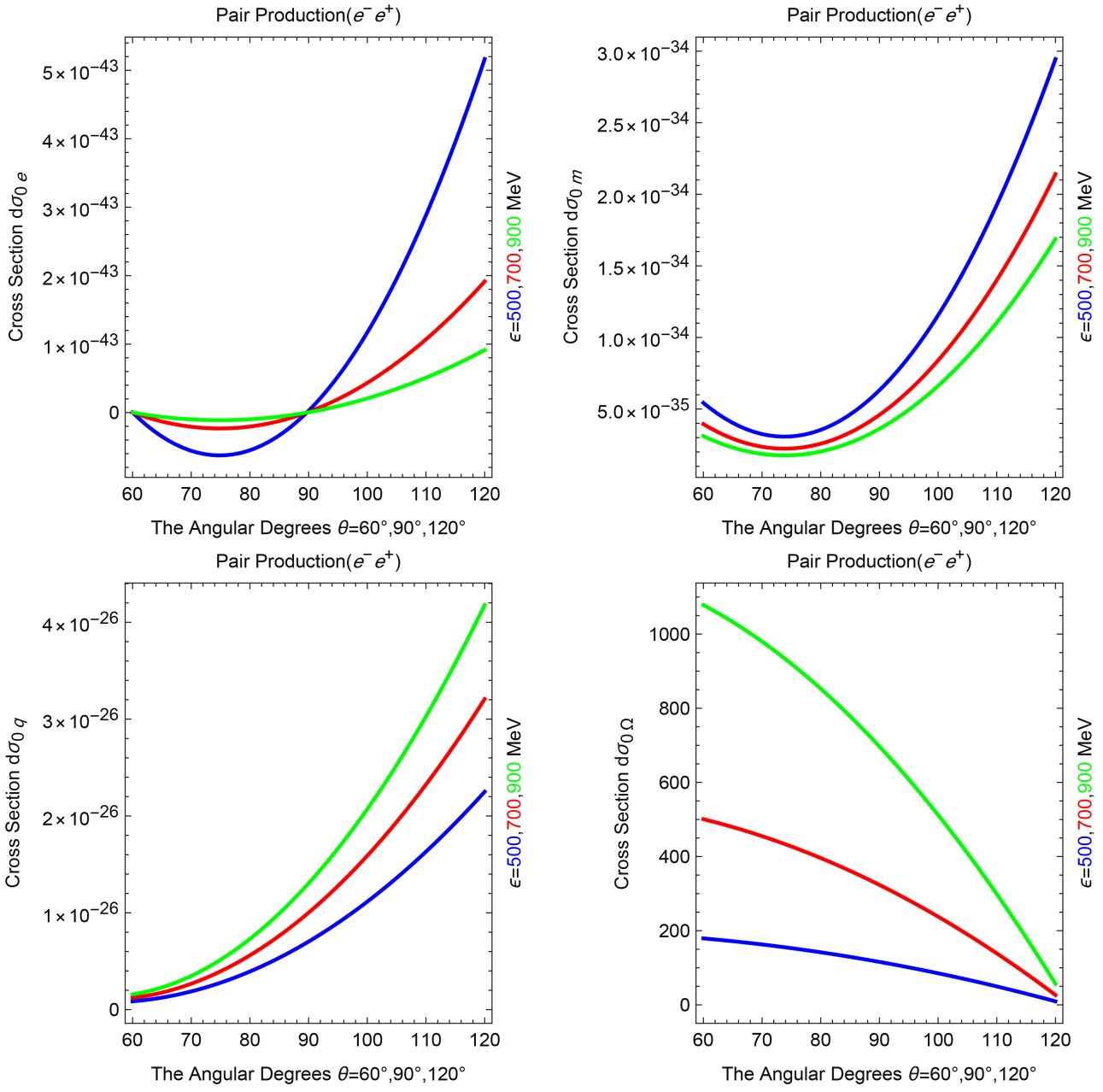

Figure 4. The DCS Electric Charge $d\sigma_{oe}$, Magnetic Dipole $d\sigma_{om}$, Electric Quadrupole $d\sigma_{oq,}$ and Magnetic Octupole $d\sigma_{o\Omega}$ for the AL_{13}^{25} nuclei.

From Figure 4 we notice that:

- The differential cross-sections electric charge $d\sigma_{oe}$ for AL_{13}^{25} nuclei are increasing with decrease the photon energy but $d\sigma_{oe}$ increases with increase the incident photon angle. For example:

The highest value at $\varepsilon = 500MeV$ and $\theta = 120^{\circ}$.

- The differential cross-sections magnetic dipole $d\sigma_{om}$ for AL_{13}^{25} nuclei are increasing with decrease the photon energy but $d\sigma_{o\mathrm{m}}$ increases with increase the incident photon angle. For example:

The highest value at $\varepsilon = 500MeV$ and $\theta = 120^{\circ}$.

- The differential cross-sections electric quadrupole $d\sigma_{oq}$ for AL_{13}^{25} nuclei are increasing with increase the photon energy but $d\sigma_{o\mathrm{q}}$ increases with increase the incident photon angle. For example:

The highest value at $\varepsilon = 900MeV$ and $\theta = 120^{\circ}$.

- The differential cross-sections magnetic octupole $d\sigma_{o\Omega}$ for AL_{13}^{25} nuclei are increasing with increase the photon energy but $d\sigma_{o\Omega}$ increases with decrease the incident photon angle. For example:

The highest value at $\varepsilon = 900MeV$ and $\theta = 60^{\circ}$

By comparing the two atoms in **Figures 3-4**, we notice that:

- For the Be_4^9 and AL_{13}^{25} nuclei, the differential cross-sections Electric Charge $d\sigma_{oe}$ and Magnetic Dipole $d\sigma_{om}$ decrease electron-positron pair production with increasing energies of the incident photons but increases with increase the incident photon angle. The highest value at $\varepsilon = 500MeV$ and $\theta = 120°$
- For the Be_4^9 and AL_{13}^{25} nuclei, the differential cross-sections Electric Quadrupole $d\sigma_{oq}$ increase electron-positron pair production with increasing energies of the incident photons but increases with decrease the incident photon angle. The highest value at $\varepsilon = 900MeV$ and $\theta = 120°$
- For the Be_4^9 and AL_{13}^{25} nuclei, the differential cross-sections magnetic octupole $d\sigma_{o\Omega}$ increase electron-positron pair production with increasing energies of the incident photons but increase with decrease the incident photon angle. The highest value at $\varepsilon = 900MeV$ and $\theta = 60°$.

4.2. Study the Effect of High Energies for Be_4^9 and AL_{13}^{25} Nuclei on the e^-e^+ Pair Production Process

By using equations (5 - 6) and different values of incident photon energies $\varepsilon = (900, 5000)\,\mathrm{MeV}$. Studies the effect of high energies in the electric quadrupole $d\sigma_{oq}$ and magnetic octupole $d\sigma_{o\Omega}$.

From **Figure 5** we notice that:

- The differential cross-sections electric quadrupole $d\sigma_{oq}$ for Be_4^9 nuclei are increasing electron-positron pair production with increasing high photons energies and increase incident photon angle. For example:

The highest value at $\varepsilon = 5000MeV$ and $\theta = 120°$.

- The differential cross-sections Magnetic Octupole $d\sigma_{o\Omega}$ for Be_4^9 nuclei are increasing electron-positron pair production with increasing high photons energies and decrease incident photon angle. For example:

The highest value at $\varepsilon = 5000MeV$ and $\theta = 60°$.

From **Figure 6** we notice that:

- The differential cross-sections electric quadrupole $d\sigma_{oq}$ for AL_{13}^{25} nuclei are

increasing electron-positron pair production with increasing high photons energies and increase incident photon angle. For example:

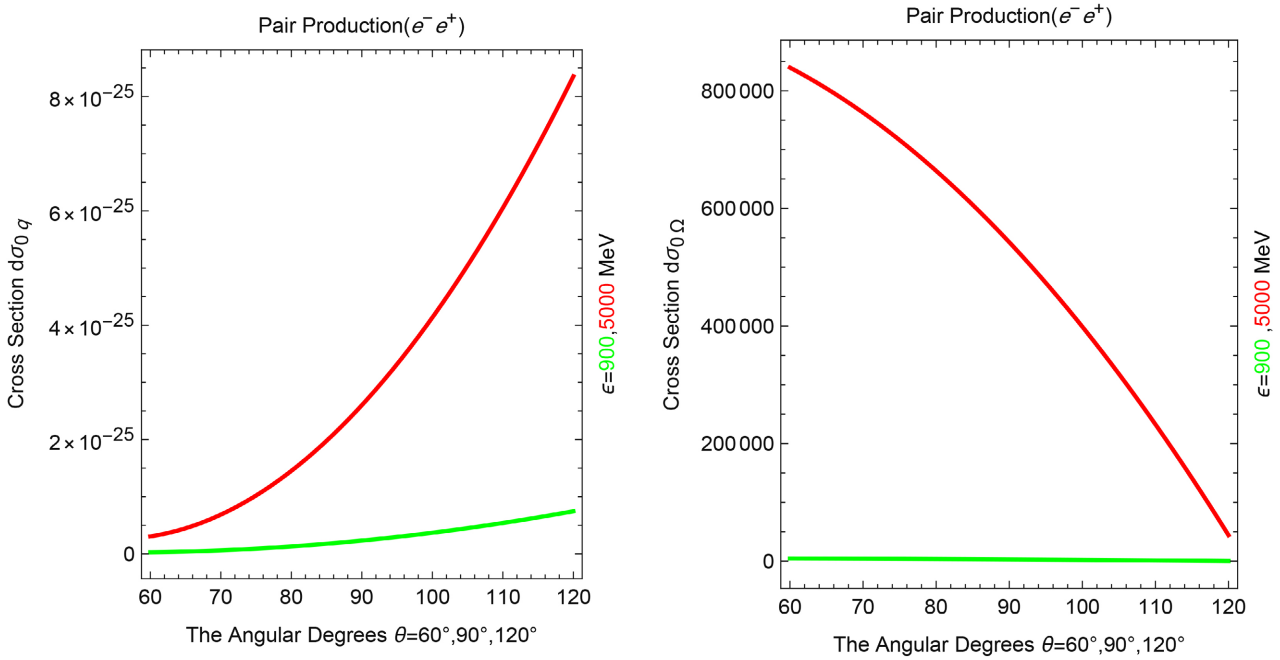

Figure 5. The DCS Electric Quadrupole $d\sigma_{oq}$ and Magnetic Octupole $d\sigma_{o\Omega}$ for the Be_4^9 nuclei.

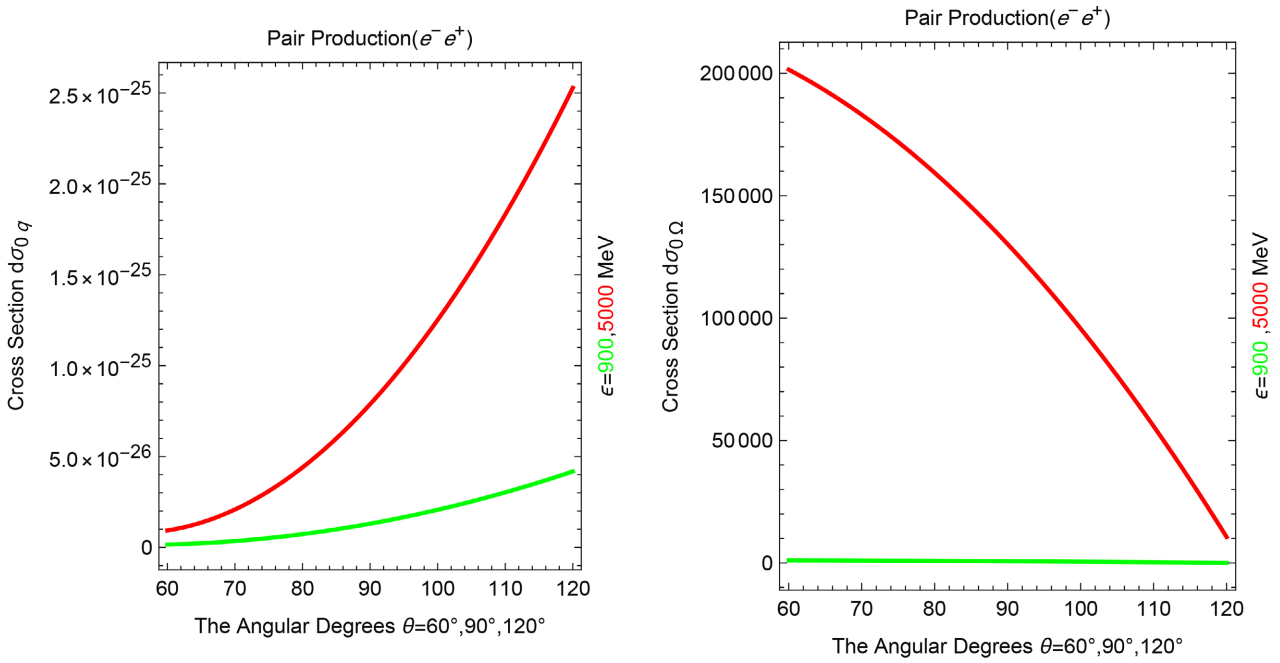

Figure 6. The DCS Electric Quadrupole $d\sigma_{oq}$ and Magnetic Octupole $d\sigma_{o\Omega}$ for the Al_{13}^{25} nuclei.

The highest value at $\varepsilon = 5000MeV$ and $\theta = 120°$.

- The differential cross-sections Magnetic Octupole $d\sigma_{o\Omega}$ for AL_{13}^{25} nuclei are increasing electron-positron pair production with increasing high photons

energies and decrease incident photon angle. For example:

The highest value at $\varepsilon = 5000MeV$ and $\theta = 60°$.

4.3. Study the Effect of Mass for Be_4^9 and AL_{13}^{25} Nuclei on the e^-e^+ Pair Production Process

From Figure 7, we notice that:

- The differential cross-sections electric quadrupole $d\sigma_{oq}$ for Be_4^9 and AL_{13}^{25} nuclei are decreasing electron-positron pair production with increasing mass nucleus. For example:

For Be_4^9

At $\varepsilon = 5000MeV$, $\theta = 120°$, $d\sigma_{oq} = 4.513966533713586 \times 10^{-25}$

For AL_{13}^{25}

At $\varepsilon = 5000MeV$, $\theta = 120°$, $d\sigma_{oq} = 2.527821258879607 \times 10^{-25}$

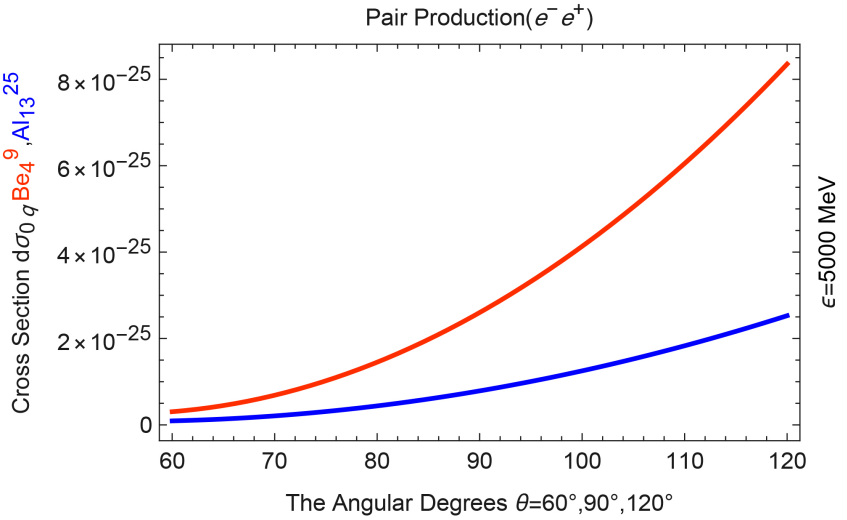

Figure 7. The DCS Electric Quadrupole $d\sigma_{oq}$ for Be_4^9 and AL_{13}^{25} nuclei.

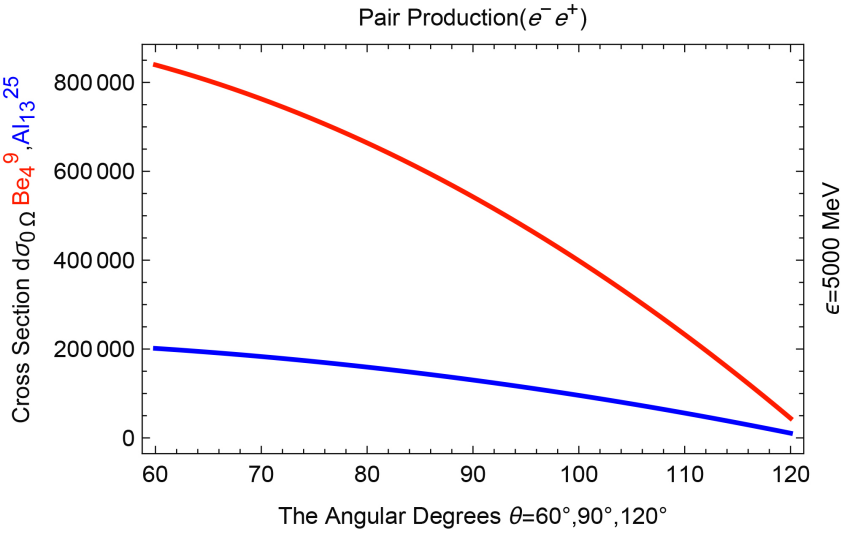

Figure 8. The DCS Magnetic Octupole $d\sigma_{o\Omega}$ for Be_4^9 and Al_{13}^{25} nuclei.

From Figure 8, we notice that:

- The differential cross-sections magnetic octupole $d\sigma_{o\Omega}$ for Be_4^9 and AL_{13}^{25} nuclei are decreasing electron-positron pair production with increasing mass nucleus. For example:

For Be_4^9

At $\varepsilon = 5000MeV$ and $\theta = 120°$ the $d\sigma_{oq} = 44198.05454852996$

For AL_{13}^{25}

At $\varepsilon = 5000MeV$ and $\theta = 120°$ the $d\sigma_{oq} = 10607.53309164719$

5. Conclusion

Our research found that in the AL_{13}^{25} and Be_4^9 nuclei, with electric charge $d\sigma_{oe}$ and magnetic dipole $d\sigma_{om}$, at an energy of 500 MeV that the formation of (e^-e^+) pairs is more efficient. In the electric quadrupole $d\sigma_{oq}$ and magnetic dipole $d\sigma_{o\Omega}$ nuclei, we have seen that at an energy of 900 MeV, the formation of (e^-e^+) pairs becomes more efficient. Moreover, for the electric quadrupole $d\sigma oq$ and the magnetic dipole $d\sigma o\Omega$, we showed that at an energy of 900 MeV, the creation of (e^-e^+) pairs becomes more effective. When looking at medium energy ε = 900 MeV and high energy ε = 5000 MeV, the creation of e^-e^+ pairs from the AL_{13}^{25} and Be_4^9 nuclei goes up at the higher energy of ε = 5000 MeV. The results indicate that lighter nuclei such that Be_4^9 produce e^-e^+ pairs more efficiently because the nuclear charge (Z) for Be_4^9 equal 4 but AL_{13}^{25} equal 13. This conclusion is consistent with observations in positron emission tomography (PET) scanners [13]. In summary, the study highlights the relationship between nuclear mass, energy levels, and multipole interactions in governing the efficiency of electron-positron pair production. The identified correlation between pair production efficiency, nuclear charge, and incident energy may have important consequences for positron emission tomography (PET). Given that positron emission tomography (PET) depends on the detection of annihilation photons from e^-e^+ pairs, understanding how lighter nuclei such as Be_4^9 favor pair production compared to heavier nuclei like AL_{13}^{25} can inform choices of target materials or tracer isotopes. Furthermore, the observed enhancement in efficiency at elevated energies indicates that optimizing energy ranges in PET systems may improve signal strength, diminish noise, and enhance image quality. Therefore, the findings offer both theoretical understanding of multipole interactions in nuclei and practical recommendations for enhancing PET technology and image analysis.

Conflicts of Interest

The authors declare no conflicts of interest regarding the publication of this paper.

References

[1] Greiner, W. and Reinhardt, J. (2008) Quantum Electrodynamics. Springer Science & Business Media.

[2] Griffiths, D. (2020) Introduction to Elementary Particles. Wiley.

[3] Wu, B. (2023) Quantum Mechanics: A Concise Introduction. Springer Nature.

[4] Nishina, Y., Tomonaga, S. and Sakata, S. (1934) On the Photoelectric Creation of Positive and Negative Electrons. Institute of Physical and Chemical Research.

[5] Bethe, H. and Heitler, W. (1934) On the Stopping of Fast Particles and the Creation of Positive Electrons. *Proceedings of the Royal Society A*, **146**, 83-112.

[6] Jaeger, J. and Hulme, H. (1936) On the Production of Electron Pairs. *Proceedings of the Royal Society A*, **153**, 443-447.

[7] Sakharov, A.D. (1948) Interaction of an Electron and Positron in Pair Production. *Journal of Experimental and Theoretical Physics*, **18**, Article 631.

[8] Hubbell, J.H. (2006) Electron-Positron Pair Production by Photons: A Historical Overview. *Radiation Physics and Chemistry*, **75**, 614-623. https://doi.org/10.1016/j.radphyschem.2005.10.008

[9] Hubbell, J.H. and Seltzer, S.M. (2004) Cross Section Data for Electron-Positron Pair Production by Photons: A Status Report. *Nuclear Instruments and Methods in Physics Research Section B: Beam Interactions with Materials and Atoms*, **213**, 1-9. https://doi.org/10.1016/s0168-583x(03)01524-6

[10] Alkhateeb, S. (2020) Effect of Nuclear Magnetic Distribution on the Photon Production of Longitudinally Polarized Lepton-Pairs in the Field of Na_{11}^{23} and Al_{13}^{27} Nuclei. *Thermal Science*, **24**, 139-147. https://doi.org/10.2298/tsci20s1139a

[11] Alkhateeb, S.A., Alshaery, A.A. and Aldosary, R.A. (2022) Electron-Positron Pair Production in Electro-Magnetic Field. *Journal of Applied Mathematics and Physics*, **10**, 237-244. https://doi.org/10.4236/jamp.2022.102017

[12] Pardy, M. (2024) The Electron-Positron Pair Production in Modern Quantum Electrodynamics.

[13] Abuelhia, E.I. (2006) The Potential Use of Three Photon Positron Annihilation Processes as a New Imaging Modality for Positron Emission Tomography (PET). University of Surrey (United Kingdom).

[14] Zhu, W. (2020) Improved Bethe-Heitler Formula. *Nuclear Physics B*, **953**, Article 114958. https://doi.org/10.1016/j.nuclphysb.2020.114958

[15] Obraztsov, I.V. and Milstein, A.I. (2021) Quadrupole Radiation and e^-e^+ Pair Production in the Collision of Nonrelativistic Nuclei. *Physics Letters B*, **820**, Article 136514. https://doi.org/10.1016/j.physletb.2021.136514